Proposal of TZT Diagram for Microstructural Analysis of Transition Zone in Dissimilar Metal Welding†

– Formation Mechanism of Austenite Coarse Grain-boundary as the Site of Disbonding between 2 · 1/4Cr-1Mo Steel and Type 309 Overlaid Metal –

Yue-Chang ZHANG*, Hiroji NAKAGAWA** and Fukuhisa MATSUDA***

Abstract

For the analysis of microstructure in the transition zone occurring in weld metal near base metal in welding dissimilar metals, Transition Zone Transformation (TZT) diagram was proposed, which gives the distribution of liquidus, solidus and transformation temperatures in the transition zone. As an example, the TZT diagrams in the transition zone between 2 · 1/4Cr-1Mo steel and type 309 overlaid metal were made on the basis of Cr and Ni distributions measured in the transition zone. Further, the combination of the TZT diagram with the temperature distribution during overlaying yielded the elucidation of formation mechanism of austenite coarse grain-boundary as the site of hydrogen disbonding. The proposed mechanism was confirmed experimentally, and could be stated as follows: The austenite (γ) grains at the fusion boundary in HAZ formed in δ → γ transformation during cooling are going to grow into the overlaid metal. Before that, however, other γ grains have already nucleated and been growing in the transition zone by the reaction of liquid → liquid + δ → liquid + δ + γ during solidification. Therefore, when the γ grains from HAZ grow only a little into the overlaid metal, both the γ grains from HAZ and in the overlaid metal collide with each other in the transition zone, and this collision makes γ grain-boundary parallel to the fusion boundary. This γ grain-boundary shifts a little accompanying the disappearing of δ during cooling, and the zone between the γ grain-boundary and the carbide layer formed after PWHT is regarded as so-called γ coarse grain.

KEY WORDS: (Stainless Steel) (Cr-Mo Steel) (Overlaying) (Disbonding) (Phase Diagram)

1. Introduction

One of the reason for difficulty in the analysis of microstructure in weld metal of dissimilar metals joint is the existence of transition zone formed near base metal. Concerning the composite region[1] where the chemical composition is nearly averaged by mixing, microstructural analysis is possible to some extent on the basis of the relevant phase diagram or Shaefler diagram for stainless steel utilizing the averaged composition evaluated from dilution ratio. In the transition zone, however, the method of microstructural analysis has not been established.

For example, the disbonding[2–18] occurring in the shutdown period of hydro-desulphurizing reactor in oil refining plants is a separation-type cracking between 2 · 1/4Cr-1Mo steel and type 309 austenitic stainless steel overlaid metal, and microscopically locates along austenite (γ) coarse grain-boundaries[3,4,13] which are formed in the transition zone in the overlaid metal. Therefore, one of the preventive measures against the disbonding is to extinguish the γ coarse grains[14]. For this purpose, high speed and high current ESW[6] and adjustment of the composition of welding materials[15] have been proposed. The formation mechanism of γ coarse grain, however, has not been revealed, and only the preventions seem to precede.

In this report, the authors would like to propose here "Transition Zone Transformation (TZT) diagram" that represents the distribution of melting point and various transformation temperatures in the transition zone of dissimilar metal joint, and to prove its effectiveness by revealing the formation mechanism of γ coarse grain-boundary from the TZT diagram in the transition zone. For this purpose, however, actual overlaying is not necessarily useful because of the instabilities or fluctuations in overlaying phenomena, as understood from the disagreement[9] among researchers concerning the effects of overlaying parameters on the formation of γ coarse grain. Therefore, in this paper the formaton of γ coarse grain is discussed mainly from the results obtained by the simulated overlaying developed newly by the authors.

† Received on April 23, 1987.
* Foreign Researcher (Shanghai Jiao Tong Univ.)
** Research Instructor
*** Professor

Transactions of JWRI is published by Welding Research Institute of Osaka University, Ibaraki, Osaka 567, Japan

2. Materials Used and Experimental Procedures

2.1 Materials used

As mentioned in the introduction, the simulated overlaying utilizing high frequency induction heating, which was developed by the authors, was mainly used, and actual overlaying was done partly for the comparison with the simulated overlaying. Type 308 stainless steel filler wire was used in the simulated overlaying so that the chemical compositions of simulated overlaid metal might equal nearly that in the first layer of the actual overlaying, because the dilution in the simulated overlaying was virtually zero, as mentioned later. The chemical compositions of 2 · 1/4Cr-1Mo steel and type 308 filler wire used in the simulated overlaying, and the first layer in the actual overlaid metal made by submerged-arc welding with type 309 strip are shown in **Table 1**. The conditions of the actual overlaying are shown in **Table 2**. Besides, **Table 3** shows the result of thermal analysis of 2 · 1/4Cr-1Mo steel and type 308 filler wire. It should be noticed that the incipient temperature of γ in type 308 filler wire during cooling is higher than that in 2 · 1/4Cr-1Mo steel.

2.2 Procedures of simulated overlaying

The apparatus of the simulated overlaying is shown in **Fig. 1**, where high frequency induction heating by one turn coil is utilized. The base metal of 2 · 1/4Cr-1Mo steel which was machined to rod shape having 7mm in diameter at the top surface, namely the overlaying surface was set to a water cooled clamp. The filler metal (3.2mm in dia. and 7 mm in length) of type 308 was hung with Pt wire. Pt/Pt-Rh thermocouple was welded on the side surface of base metal at 1 mm below from the overlaying surface. The base metal was heated in Ar gas atmosphere (99.999%) under the heating rate of about 60°C/sec, and after the attainment to a peak temperature (T_p) the filler metal was brought near to the induction coil to be melted, and dropped on the overlaying surface of base metal. An example of the thermal cycle is shown in **Fig. 2**. Generally, T_p was set to 1380°C. During heating, the temperature difference between the overlaying surface and the place of the thermocouple was about 10°C.

At the instant of the drop of melted filler metal, the temperature at the thermocouple was increased a little as seen in Fig. 2, and then was cooled in a programmed rate. Namely, referred to the mean cooling rate between 1400 and 1000°C in the actual overlaying by ESW[16], the cooling rate of 10°C/sec as standard one and other cooling rates of 2 and 40°C/sec were selected. When the temperature was cooled down to 1350°C, it was observed with the naked eye that the overlaid metal started to solidify from the overlaying interface. This temperature has a difference of about 100°C from the melting point of type 308 filler metal shown in Table 3. This means that there was about 100°C difference between the overlaying interface and the place of thermocouple during cooling. In other words, there was a temperature gradient of about 100°C/mm during cooling near the overlaying interface.

According to the microscopic observation of many specimens, traces of tooling on the overlaying surface remained at the overlaying interface after the simulated overlaying. This means that the dilution of base metal was virtually zero. Consequently, it was judged that the chemical composition of the simulated overlaid metal was almost the same as that of type 308 filler metal.

After the overlaying, the specimen was heat-treated at 690°C × 20 hr to make the observation of γ coarse grain clear utilizing carbides precipitation on the grain-boundary, because it was established that the γ coarse grain is formed in as-welded condition, and not by PWHT[15].

Distribution of Cr and Ni concentrations in the transition zone was measured by EDX line analysis, where the concentrations were calibrated from the cps value of the

Table 1 Chemical compositions of materials used

Material		Chemical composition (wt.%) C	Si	Mn	P	S	Cr	Ni	Mo	Remarks
Simulated overlaying	2 1/4 Cr-1Mo plate	0.09	0.19	0.50	0.005	0.003	2.22	-	0.99	25mm thick.
	308 wire	0.06	0.37	1.81	0.024	0.001	19.92	10.17	-	3.2mm dia.
Actual overlaying	2 1/4 Cr-1Mo plate	0.13	0.16	0.54	0.005	0.004	2.39	-	1.05	115mm thick.
	309 overlaid metal	0.05	0.58	1.40	-	-	19.51	9.40	0.24	first layer

Table 2 Conditions of actual overlaying by SAW

Welding current (A)	Arc voltage (V)	Welding speed (mm/sec)
1200	27	2.5

Filler metal: 75mm width x 0.4mm thickness

Table 3 Results of thermal analysis

Material	Liquidus (°C)	$T_{\gamma i}$* (°C)
2 1/4Cr-1Mo steel	1512	1403
type 308 wire	1446	about 1430

* $T_{\gamma i}$: Incipient temperature of austenite during cooling

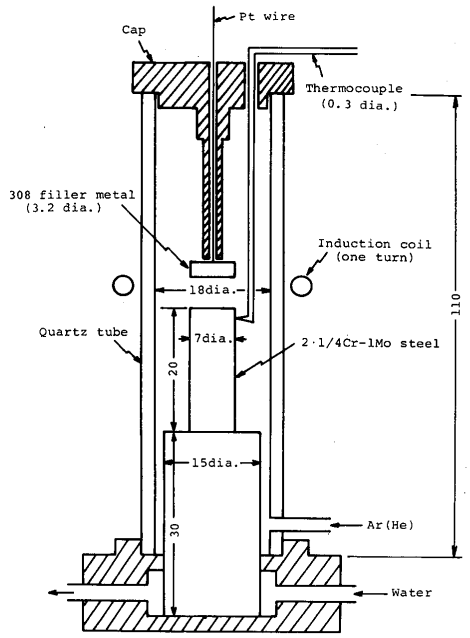

Fig. 1 Equipment for simulated overlaying by induction heating

base metal and the filler metal.

2.3 Definition of ratio of γ coarse grain

The ratio of the number of γ coarse grains in the transition zone to the number of prior γ grains in HAZ adjacent to the overlaying interface was defined as the ratio of γ coarse grain. These numbers were measured over 7 mm along the overlaying interface.

3. Concept of Transition Zone Transformation (TZT) Diagram and Proposed Formation Mechanism of γ Coarse Grain

3.1 Correspondence of microstructure between actual and simulated overlaid metal

Figure 3 compares the γ coarse grains in (a) the actual overlaying and (b) the simulated overlaying (T_p: 1380°C, cooling rate: 2°C/sec) with each other. In both cases, δ phases are hardly observed in the γ coarse grain, but frequently in the outside of the γ coarse grain as seen in the general microstructure in the composite region.

Then, Cr and Ni distributions in the transition zone measured perpendicularly to the overlaying interface, namely the fusion boundary were compared with each other. **Figure 4** shows the distribution of Cr in (a) the actual overlaying, the simulated overlaying under (b) cooling rate of 10°C/sec after T_p of 1380°C and (c) cooling rate of 2°C/sec after T_p of 1380°C, where the solid and the broken lines mean they were measured in the parts with and without γ coarse grain, respectively. Especially, the thick part of the solid line indicates the

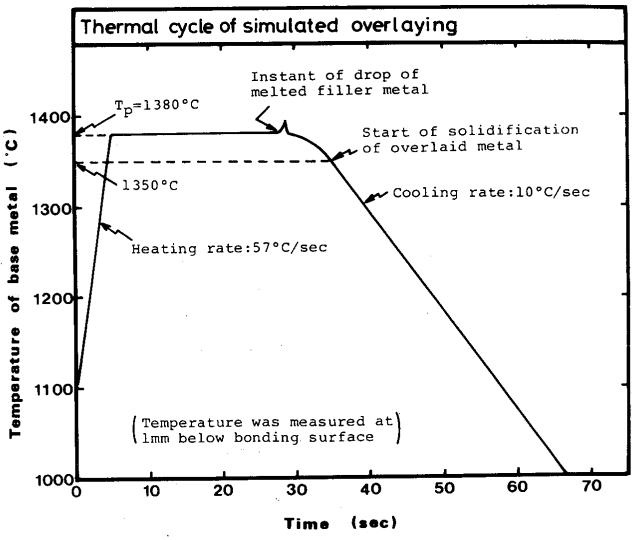

Fig. 2 An example of thermal cycle during simulated overlaying

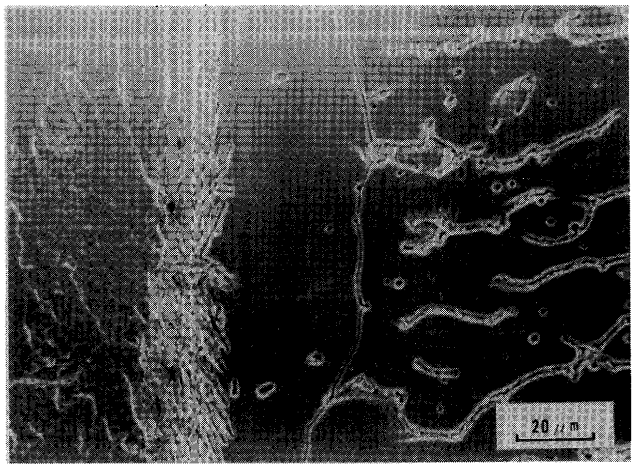

(a) actual overlaying

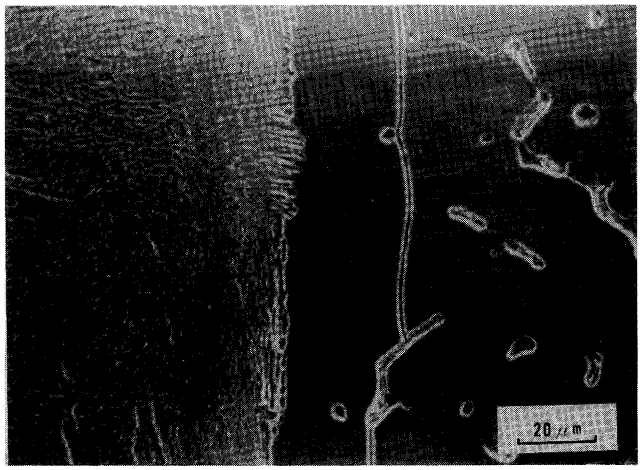

(b) simulated overlaying

Fig. 3 Comparison of γ coarse grain between actual and simulated overlaying

region of γ coarse grain, in which its inner limit corresponds to the outer limit of carbide layer. It is seen from every distribution that the Cr concentration in the γ coarse grain was a little lower than the part without γ

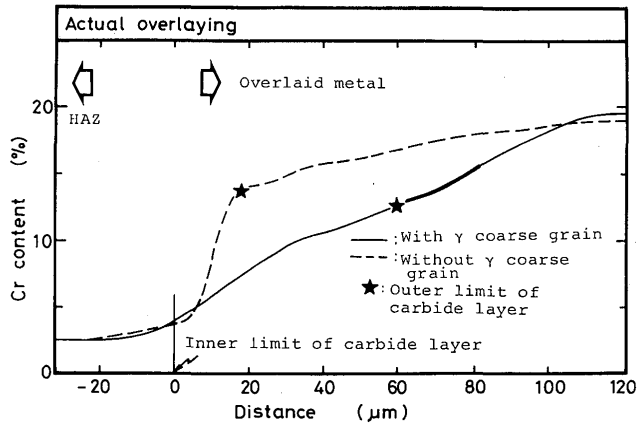

(a) actual overlaying

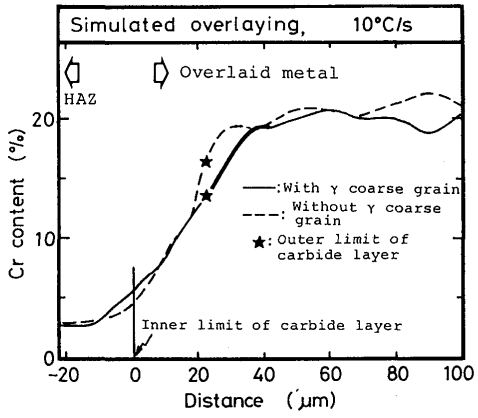

(b) simulated overlaying (10°C/sec)

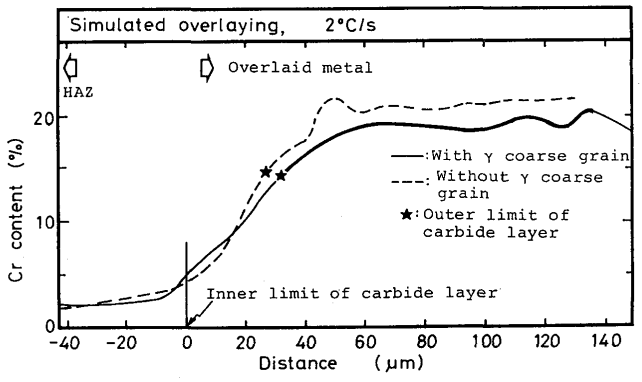

(c) simulated overlaying (2°C/sec)

Fig. 4 Distribution of Cr in transition zone

coarse grain. The similar results were obtained about Ni distribution.

Therefore, it is understood that the microstructures in the simulated overlaying agree well with those in the actual overlaying.

3.2 Concept of TZT diagram

It was once presumed[4,10,16] that γ coarse grain is formed by epitaxial growth from HAZ in the manner of planar solid-liquid interface at solidification. Yasuda, et al.[5,9], however, pointed out that γ coarse grain-boundaries intersect with dendritic subboundaries, and thus stated that it is not formed at solidification. This suggests that γ coarse grain is formed in the transformation from delta (δ) to γ.

In order to discuss any transformation process in detail, at least the transformation temperatures including melting point should be known. However, in the transition zone formed in dissimilar metal welding such as overlaying, the chemical composition changes gradually as seen in Fig. 4, and this means that also the transformation temperatures change gradually. In such case, it is very difficult to assess these temperatures. Fortunately, it is well appreciated to discuss the solidification mode in weld metal of stainless steels by approximating them to Fe-Cr-Ni ternary alloys. Therefore, it may be reasonable to expect that the distribution of transformation temperatures in the transition zone can be assessed by applying the distributions of Cr and Ni measured to Fe-Cr-Ni phase diagram[19] with approximating base metal to Fe-2 · 1/4Cr alloy.

Figure 5 shows the distributions of liquidus, solidus, $\delta \rightarrow \delta + \gamma$ and $\delta + \gamma \rightarrow \gamma$ transformation temperatures in the transition zone with γ coarse grain shown in Fig. 4(a) in the actual overlaying, where Ni distribution was measured separately. The abscissa means the distance from the fusion boundary to the inside of overlaid metal, and the origin was set to the inner limit of the carbide layer. In principle, the origin should be set to the fusion boundary, but the identification was impossible because it was difficult to etch dendritic structure due to the carbide layer. The fusion boundary on the abscissa was indicated for convenience as the position where there was no influence of composition from the filler metal. It is thought that the actual fusion boundary located at a little right side. Such figure as Fig. 5 is named hereafter Transition Zone Trans-

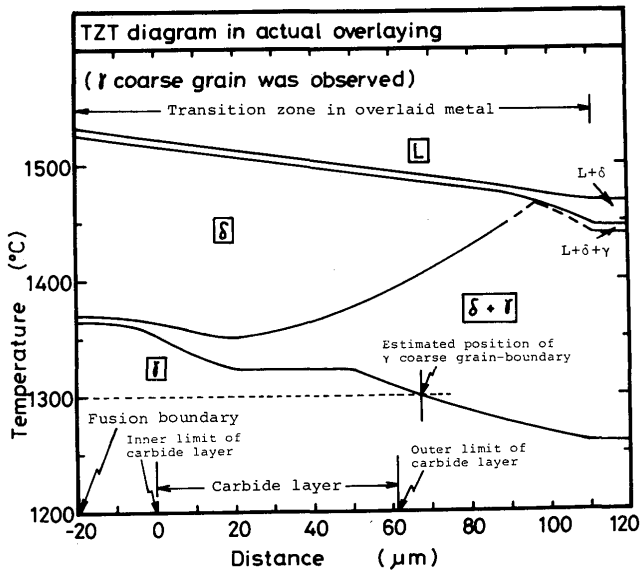

Fig. 5 An example of TZT diagram in actual overlaying (in this part, γ coarse grain was observed.)

formation (TZT) diagram. The right border in Fig. 5, namely the composite region means the solidification proceeds as liquid (L) → L + δ → L + δ + γ → δ + γ, and this prediction agrees well with that known in usual solidification mode in type 304–309 austenitic stainless steels. Moreover, it is understood that the transition zone except the part near the composite region solidifies as single δ phase. The liquidus, the solidus and the δ + γ → γ boundary lines fall nearly monotonously together with the distance, but the δ → δ + γ boundary line shows once a minimum, then rises again to a maximum, and again falls a little near the composite region. Therefore, the characteristics of solidification and the subsequent transformation in the transition zone can be well recognized from TZT diagram.

3.3 Proposed formation mechanism of γ coarse grain from TZT diagram

According to Fig. 5, it is noticed that the maximum temperature of δ → δ + γ boundary line locates in the transition zone near the composite region. This suggests that before the growth of γ grains from HAZ into the overlaid metal, other γ grains have already nucleated in the transition zone, and that the γ coarse grain-boundaries are formed by the collision of these γ grains. In order to complete this idea, the temperature distribution during overlaying is required, and thus the detailed mechanism is discussed in the following on the basis of the TZT diagram combined with the temperature gradient measured in the simulated overlaying.

Figure 6 shows the TZT diagram in the transition zone corresponding to the solid line in Fig. 4 (c), namely in the part with γ coarse grain under the cooling rate of 2°C/sec. General characteristics of this TZT diagram is the same as that in Fig. 5, and it is seen that the incipient temperature of γ in the composite region is higher than that in HAZ, agreeing with the results in Table 3.

Figure 6 also includes the temperature distribution T_1 to T_9 at different stages during cooling on the basis that the temperature gradient during cooling was about 100°C/mm. The combination of the TZT diagram with T_1 to T_9 yields next descriptions of the sequence of solidification and transformation processes and thus the formation mechanism of γ coarse grain-boundary, which are also illustrated in **Fig. 7**.

T_1: δ starts to solidify from the fusion boundary. T_2: δ grows epitaxially into the overlaid metal. T_3: γ starts to form at the part of the maximum temperature of δ → δ + γ boundary in the overlaid metal, which nearly corresponds to the boundary between the transition zone and the composite region. Microscopically, γ is formed near the boundaries between δ dendrites. T_4: γ grows in two directions. Namely, γ grows into the composite

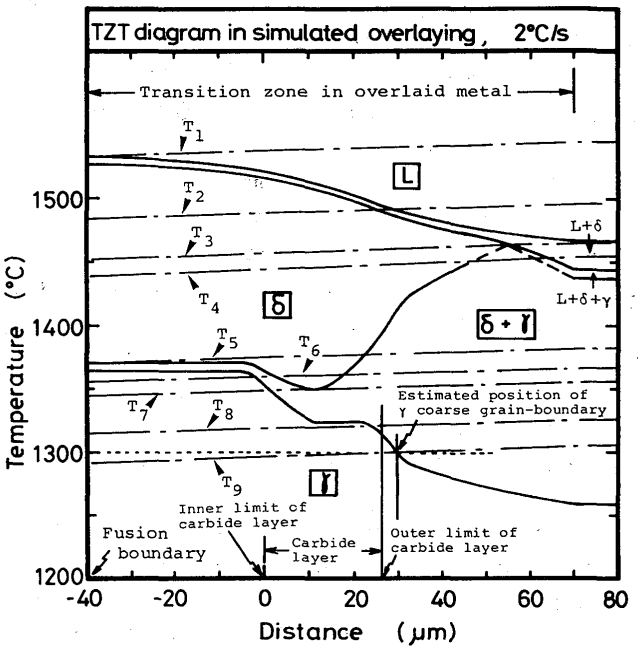

Fig. 6 An example of TZT diagram in simulated overlaying (in this part, γ coarse grain was observed.)

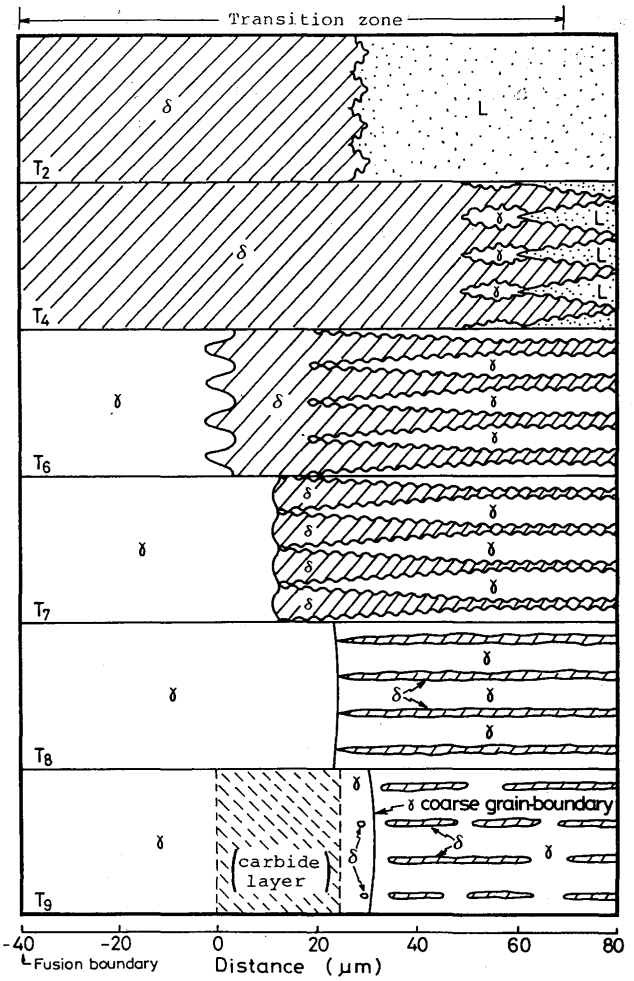

Fig. 7 Illustration of solidification and transformation sequence in the transition zone corresponding to Fig. 6

region in the overlaid metal together with δ solidifying, and also grows toward HAZ according to the characteristic of $\delta \rightarrow \delta + \gamma$ boundary line in the TZT diagram. T_5: Another γ starts to grow also from the fusion boundary. T_6: In the transition zone, the growing direction of both γ from the overlaid metal and from the fusion boundary face on each other. T_7: Both γ collide against each other at about 1350°C. Further, the phase boundary between γ from HAZ and δ changes to γ grain-boundary because of disappearance of δ at this boundary as read in the TZT diagram. T_8: The γ grain-boundary shifts toward the composite region accompanying the disappearance of δ according to the characteristic of $\delta + \gamma \rightarrow \gamma$ boundary. T_9: The shift of γ grain-boundary stops at a limit temperature discussed next.

The reason why a limit temperature was postulated in T_9 is as follows: In the right edge in Fig. 6, namely the composite region, δ formed at solidification must decrease gradually to zero at about 1260°C during cooling. However, the well known fact that there are retained δ of several percent at room temperature in the composite region as seen in Fig. 3 means that the diffusion for $\delta \rightarrow \gamma$ transformation near 1260°C is not enough under the continuous cooling condition*. Because the shift of γ grain-boundary is considered to accompany the disappearance of δ, there should be a limit temperature above 1260°C where the shift of γ grain-boundary stops. Considering the experimental results mentioned later, the limit temperature was postulated to be 1300°C. Namely in the following discussion, the intersection of $\delta + \gamma \rightarrow \gamma$ boundary line with 1300°C gives the stop position of γ grain-boundary.

Now, also the position of carbide layer is drawn in Fig. 6, and it is noteworthy that the γ grain-boundary stopped at 1300°C locates at the outside of the carbide layer. Therefore, the zone between the γ grain-boundary and the carbide layer can be regarded as so-called γ coarse grain. Namely saying simply, the formation mechanism of γ coarse grain can be explained as follows: The γ grains at the fusion boundary in HAZ formed in $\delta \rightarrow \gamma$ transformation during cooling are going to grow into the overlaid metal. Before that, however, other γ grains have already nucleated and been growing in the transition zone near the composite region by the reaction of liquid → liquid + δ → liquid + δ + γ during solidification. Therefore, when the γ grains from HAZ grow only a little into the overlaid metal, both the γ grains from HAZ and in the overlaid metal collide with each other in the transition zone at about 1350°C, and this collision makes γ grain-boundary parallel to the fusion boundary. This γ grain-boundary shifts a little accompanying the disappearance of δ during cooling in 1350 to 1300°C, and the zone between the γ grain-boundary and the carbide layer after PWHT is regarded as so-called γ coarse grain.

Also in the TZT diagram in the actual welding shown in Fig. 5, the intersection of $\delta + \gamma \rightarrow \gamma$ boundary line with 1300°C locates at the outside of the carbide layer, agreeing with the situation in Fig. 6.

4. Experimental Confirmation of Formation Mechanism of γ Coarse Grain

4.1 Study on formation temperature of γ coarse grain by quenching

Specimen was quenched with He gas at various stage during the cooling in the simulated overlaying. The ratio of γ coarse grain measured vs. the quenching temperature is shown in **Fig. 8**. There was no γ coarse grain in the specimens quenched at 1350, 1300 and 1250°C. On the other hand, γ coarse grains were observed in the specimens quenched at 1200 and 1100°C. Considering the temperature difference of about 100°C between the overlaying interface and the position of thermocouple mentioned in 2.2, it is reasonable to conclude that γ coarse grain is formed at about 1350 to 1300°C, and this agrees well with the temperature where both γ from HAZ and in the overlaid metal collide with each other or the disappearance of δ is stopped in Fig. 6.

The microstructures quenched at 1300 and 1200°C are shown in **Fig. 9**. In (a) quenched at 1300°C, γ coarse grain is not seen, and rather many δ phases are seen from the vicinity of carbide layer. This is because of the suppression of disappearance of δ phase even in the transition zone near HAZ by quenching, and supports that the formation of γ coarse grain is connected with the shift of γ grain-boundary following the disappearing process of δ at about 1350 to 1300°C. Besides, by comparing the location of δ

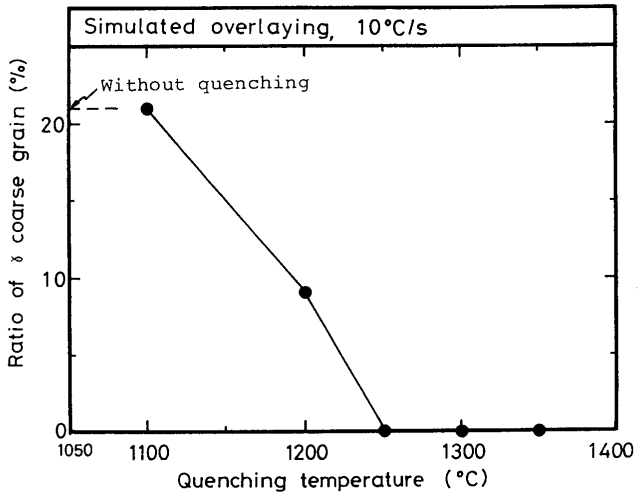

Fig. 8 Effect of quenching temperature on ratio of γ coarse grain

*) There is a report[20] claiming that δ is decreased by massive transformation of γ, but it seems unlikely[21].

(a) quenched at 1300°C

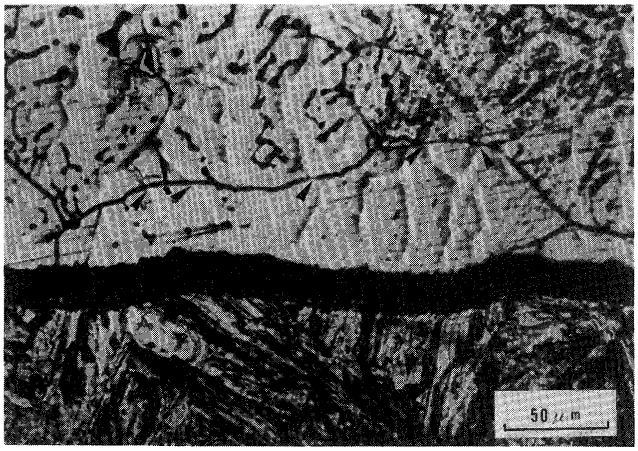

(b) quenched at 1200°C (arrows mean intersection of γ coarse grain-boundary with solidification sub-boundary

Fig. 9 Effect of quenching during cooling after solidification on microstructure

phase with dendrite or cell boundaries which are observed as depressions in (a), it is understood that δ phases are at the core of dendrite or cell. This means that the solidification in the overlaid metal including the transition zone occurred as primary δ, agreeing with the TZT diagram. In (b) quenched at 1200°C, it is observed that the dendrite or cell boundaries indicated by triangular arrows intersect with the γ coarse grain-boundary, agreeing with the result by Yasuda[5,9]. Also this confirms that γ coarse grain is not formed at solidification.

4.2 Feature of microstructure and TZT diagram in the part having no γ coarse grain

In the transition zone where there was no γ coarse grain in the actual and the every simulated overlaid metal, δ phases are formed readily from the vicinity of carbide layer as shown in **Fig. 10**.

Also this can be explained from the TZT diagram as follows: **Figure 11** shows the TZT diagram in the transition zone corresponding to the broken line in Fig. 4 (a), namely in the part without γ coarse grain in the actual

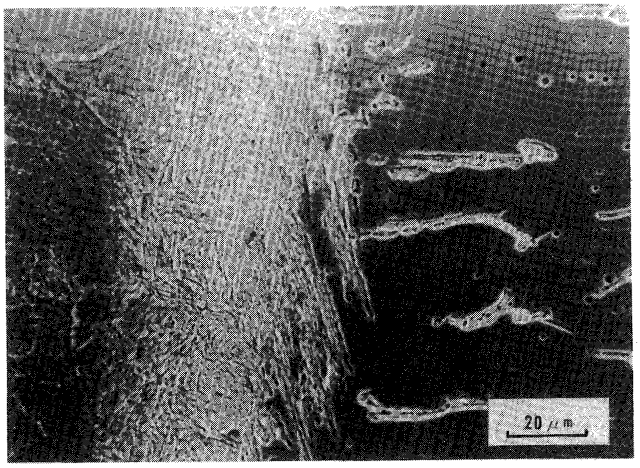

Fig. 10 Microstructure near carbide layer in the part where no γ coarse grain was formed in actual overlaying

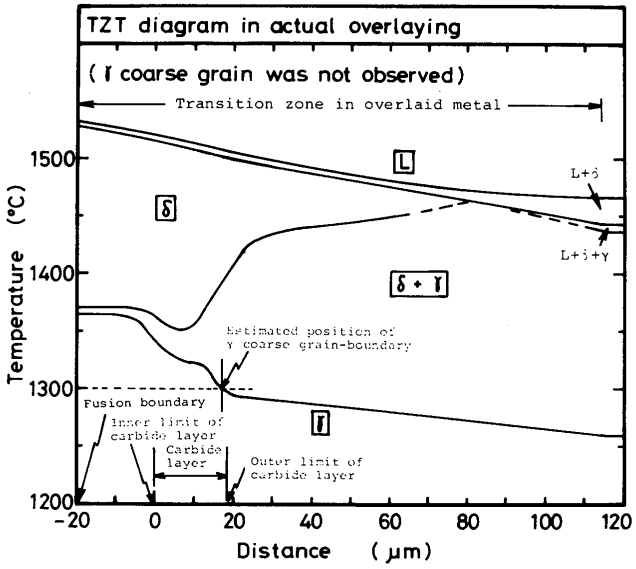

Fig. 11 An example of TZT diagram in actual overlaying (in this part, no γ coarse grain was observed.)

overlaying. It is noticed that the intersection of $\delta + \gamma \rightarrow \gamma$ boundary line with 1300°C locates inside of the carbide layer. The same relation was also seen in the TZT diagram in the simulated overlaying. This suggests that in the transition zone where no γ coarse grain was seen γ grain-boundary only stopped at a position being inside the carbide layer. Although it is generally difficult to observe γ grain-boundary as the prior γ grain-boundary in the carbide layer due to its complex microstructure, the evidence confirming that there was prior γ grain-boundary in carbide layer in the parts where no γ coarse grain was seen was sometimes obtained, and one of the example is shown in **Fig. 12.**

4.3 Effect of width of transition zone on formation of γ coarse grain

According to the above experimental results, the proposed mechanism of γ coarse grain from TZT diagram was

nearly proper. On the other hand, it seems that there is not necessarily any agreement among researchers on the effects of overlaying processes or parameters on the formation of γ coarse grain. In the following, the effect of cooling rate as a relevant variable is discussed, and interpreted from the viewpoint of the width of transition zone.

The relation between the cooling rate and the ratio of γ coarse grain is shown in **Fig. 13**. The ratio decreased with an increase in the cooling rate and disappeared at cooling rate of 40°C/sec. The microstructure at 40°C/sec was nearly the same as that quenched at 1300°C shown in Fig. 9 (a), and means that the disappearing process of δ in the transition zone was suppressed by the high cooling rate. On the other hand, the ratio of γ coarse grain at 10°C/sec is fairly different from that at 2°C/sec, although the amount and morphology of δ phases at these two cooling rates were nearly the same as each other. Because δ is decreased by diffusion controlled transformation, the fact that there was little difference in δ phases between these two cooling rates suggests that there was little difference in the extent of diffusion controlled transformation causing extinguishing process of δ in the two cooling rates. Therefore, it is thought that the difference in the ratio of γ coarse grain in these cooling rates were due to another factor. For example, it should be reasonable that the width of transition zone affects the ratio, because γ coarse grain is formed inside the transition zone. Comparing Fig. 4 (b) with (c), it is noticed that the concentration gradient at 2°C/sec is wider than at 10°C/sec. Therefore, it is thought that the cooling rate affects indirectly the ratio of γ coarse grain through its effect on the width of transition zone.

Thus, melting time, namely the contacting time of melted overlaid metal with the base metal which is considered to affect the width of transition zone directly was studied. Under general thermal cycle mentioned in 2.2, the melting time was about 6 and 14 sec at the cooling rates of 10 and 2°C/sec, respectively. Furthermore, at 10°C/sec it was possible to lengthen the melting time to about 17 sec without detectable dilution of base metal. The ratio of γ coarse grain under these melting times are shown in **Fig. 14**, where the ratio has a linear correlation with the melting time irrespective of the cooling rate. Therefore, it is understood that the width of transition zone formed in the melting state, in other words the distribution of alloying element is one of the major factor of γ coarse grain.

The reason why the wide transition zone promotes the formation of γ coarse grain is that the intersection of $\delta + \gamma \rightarrow \gamma$ boundary line with 1300°C gradually goes away more and more from the fusion boundary with the widening of transition zone, as seen from the comparison between Figs. 5 and 11. Yasuda, et al.[9] showed that the

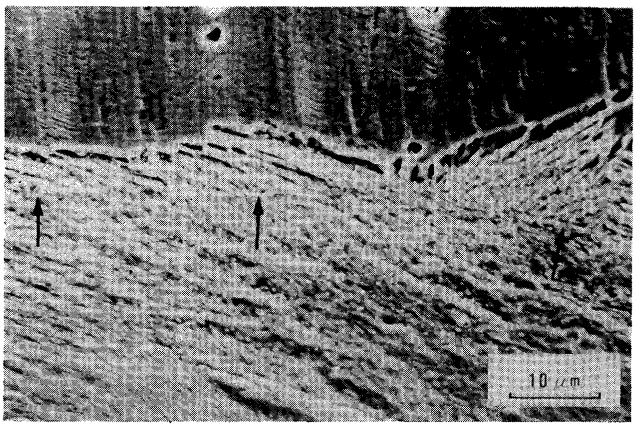

Fig. 12 An example of prior γ grain-boundary observed in carbide layer, indicated by arrows

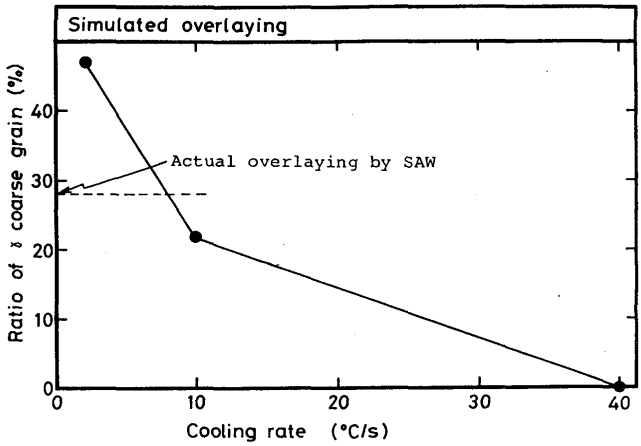

Fig. 13 Effect of cooling rate on ratio of γ coarse grain

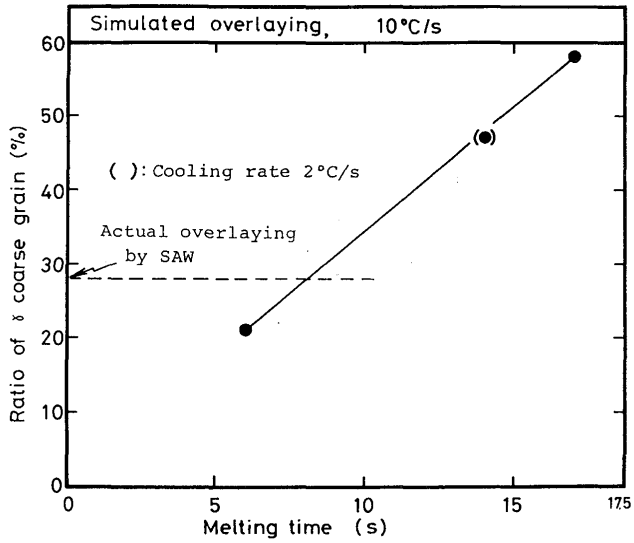

Fig. 14 Effect of melting time on ratio of γ coarse grain

formation of γ coarse grain has a good correlation with welding speed irrespective of overlaying procedure, and this effect of welding speed may be attributed to the effect of melting time during overlaying.

Someone may claims that the differentia between the parts with and without γ coarse grain is the difference in

Cr/Ni ratio, because Cr and Ni are delta and austenite stabilizers, respectively. Concerning this problem, **Fig. 15** plots the Cr-Ni relation in the transition zone on Fe-Cr-Ni phase diagram, and means that there was little difference in Cr-Ni relation or Cr/Ni ratio between the parts with and without γ coarse grain.

4.4 Effect of solidification mode on formation of γ coarse grain

One of the point in the proposed formation mechanism of γ coarse grain is that before the growth of γ grains from HAZ into the overlaid metal, other γ gains have been already formed in the transition zone. This is further confirmed by supercooling the overlaid metal including the transition zone. Namely, type 304 to 309 austenitic stainless steels generally solidifies as primary δ, but as primary γ by an increase in supercooling or cooling rate[18,19]. Therefore, if T_p is set to a low temperature so that the temperature of the overlaying interface may be always in γ zone in spite of the sudden rise in temperature due to the drop of melted filler metal, the γ grains in HAZ will solidify epitaxially into the overlaid metal which also solidifies as primary γ because of the very high cooling rate in the solidification range. Consequently, γ coarse grain that has grain-boundary parallel to the fusion boundary will not be formed, because the γ grains solidifying epitaxially from HAZ will have elongated grain-boundaries perpendicular to the fusion boundary.

The prediction is confirmed in **Fig. 16**, where the ratio of γ coarse grain is plotted against T_p. The ratio in the case of T_p = 1360°C was nearly the same as that in T_p = 1380°C. However, the ratio in the cases of T_p = 1320 and 1300°C was zero, namely no γ coarse grain was formed. The microstructure in T_p = 1300°C shown in **Fig. 17** confirms that the overlaid metal solidified as primary γ judging from the fact that δ phases were formed at dendrite or cell boundaries as depressions, and also confirms that the prior γ grain-boundaries in HAZ grew to the γ grain-boundaries in the overlaid metal in an elongated manner nearly perpendicular to the fusion boundary as indicated by arrows.

Therefore, γ coarse grain is not formed when the overlaid metal including the transition zone solidifies as primary γ. Also this supports the statement in 3.3 that the formation of γ coarse grain is connected with the disappearing process of δ after solidification.

4.5 Interpretation of preventive measures of γ coarse grain from TZT diagram

Ohnishi, et al.[6] showed that high speed and high current ESW is effective to prevent the disbonding. In this technique, γ coarse grains are suppressed, although the reductions of accumulated hydrogen content and residual

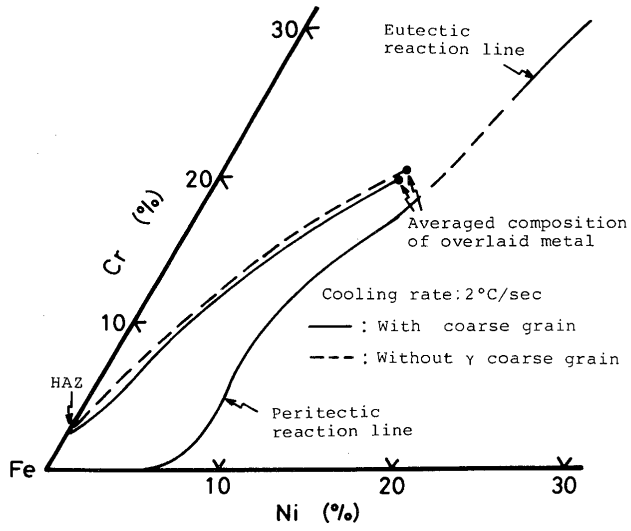

Fig. 15 Comparison of Cr-Ni relation in transition zone between cases with and without γ coarse grain

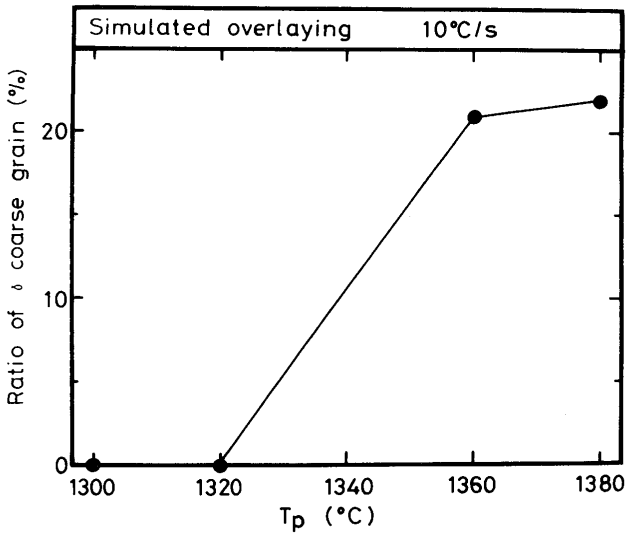

Fig. 16 Effect of peak temperature of base metal on ratio γ coarse grain

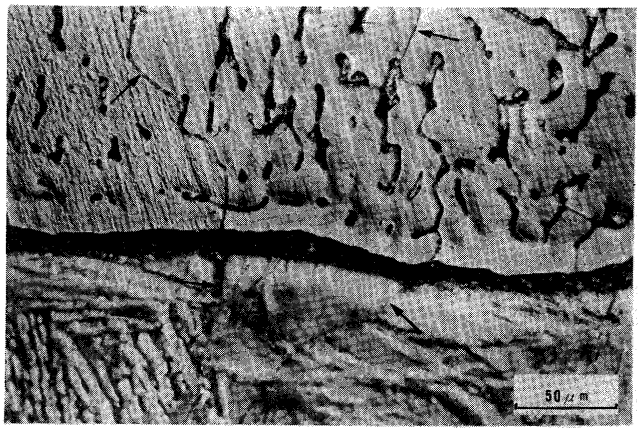

Fig. 17 Microstructure in peak temperature of 1300°C, showing γ in HAZ growing epitaxially owing to solidification mode of primary γ

stress due to γ + martensite structure in the overlaid metal are other reasons[6]. In the following, the reason for the

suppression of γ coarse grain is discussed on the basis of its TZT diagram. According to their report[6], the major composition under the high speed and high current ESW is about 15%Cr-8%Ni because of large dilution of base metal. The TZT diagram in this case is shown in **Fig. 18** on the basis of an imaginary Cr and Ni distribution in the transition zone drawn in the upper part in Fig. 18. The characteristic of $\delta \rightarrow \delta + \gamma$ boundary line is nearly the same as that in Fig. 6. It is noteworthy, however, that $\delta + \gamma \rightarrow \gamma$ boundary line is always above 1350°C. Therefore, it is guessed that the shift of γ grain-boundary occurring at T_7 to T_9 in Fig. 6 is not stopped, and thus the γ grain-boundary paralleling the fusion boundary is hardly formed inside the transition zone.

On the other hand, Yasuda, et al.[15] showed that utilizing welding materials yielding higher δ content in overlaid metal is effective to prevent the disbonding by confining the γ coarse grain-boundary inside the carbide layer. In the following, the reason for the confinement of γ coarse grain is discussed on the basis of its TZT diagram. The major composition in this case is about 21%Cr-9%Ni[24], and the TZT diagram is shown in **Fig. 19** on the basis of an imaginary Cr and Ni distribution in the transition zone in the upper part in Fig. 19. Figure 19 means that the overlaid metal including the transition zone solidifies as only primary δ phase, and γ is formed after the completion of solidification, which agrees with the report by Yasuda[15]. It is noteworthy that the temperature of $\delta + \gamma \rightarrow \gamma$ boundary line drops suddenly below 1300°C in the vicinity of fusion boundary. Therefore, it is guessed that the shift of γ grain-boundary is soon stopped, and thus the γ grain-boundary locates in the carbide layer formed after PWHT.

As mentioned above, TZT diagram is very useful for the interpretation of not only the formation mechanism but also the preventive measures of γ coarse grain-boundary.

However, the distance from the fusion boundary to the γ coarse grain-boundary in the actual cases was longer than the prediction from the TZT diagram. The reason of this difference is thought to be neglecting the effects of other alloying elements and non-equilibrium cooling condition in TZT diagram, and to be the assumption that the limit temperature of disappearing process of δ is always 1300°C. The selection of this limit temperature influences the stopping position of γ grain-boundary effectively.

5. Conclusions

Transition Zone Transformation (TZT) diagram was proposed for the microstructural analysis of transition zone in dissimilar metals welding. The effectiveness was shown by revealing the formation mechanism of γ coarse grain in the transition zone in type 309 overlaid metal on 2 · 1/4Cr-1Mo steel. Main conclusions obtained are as follows:

(1) For the transition zone in type 309 overlaid metal on 2 · 1/4Cr-1Mo steel, TZT diagram was completed by plotting the Cr and Ni distributions measured in the transition zone on Fe-Cr-Ni phase diagram, and useful to understand the distributions of liquidus, solidus and various transformation temperatures and solidifi-

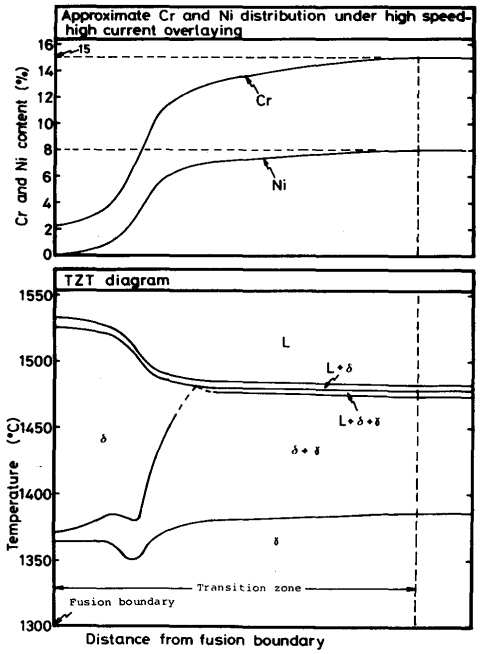

Fig. 18 TZT diagram under high speed-high current overlaying of 309

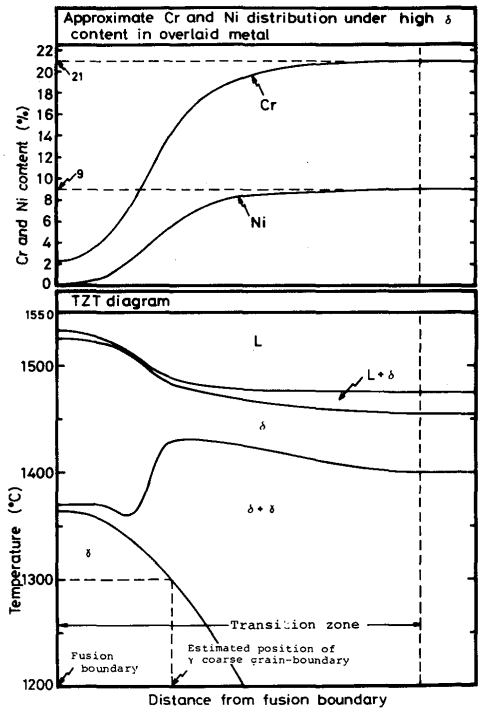

Fig. 19 TZT diagram in overlaying of filler metal yielding high δ content

cation mode in the transition zone.

(2) Formation mechanism of γ coarse grain could be interpreted from the TZT diagram combined with the temperature distribution, and is expressed simply as follows: The γ grains at the fusion boundary in HAZ formed in $\delta \rightarrow \gamma$ transformation during cooling are going to grow into the overlaid metal. Before that, however, other γ grains have already nucleated and been growing in the transition zone near the composite region by the reaction of liquid $\rightarrow$ liquid + $\delta \rightarrow$ liquid + δ + γ during solidification. Therefore, when the γ grains from HAZ grow only a little into the overlaid metal, both the γ grains from HAZ and in the overlaid metal collide with each other in the transition zone at about 1350°C, and this collision makes γ grain-boundary parallel to the fusion boundary. This γ grain-boundary shifts a little accompanying the disappearance of δ during cooling in 1350 to 1300°C, and the zone between the γ grain-boundary and the carbide layer after PWHT is regarded as so-called γ coarse grain.

(3) It was confirmed experimentally that γ coarse grain is not formed at solidification, but at $\delta + \gamma \rightarrow \gamma$ transformation in about 1350 to 1300°C, which supported the proposed mechanism from the TZT diagram.

(4) Long contacting time of melted overlaid metal with base metal promotes the formation of γ coarse grain. In other words, wide transition zone promotes the formation of γ coarse grain. Also this tendency could be explained from the characteristic of TZT diagram.

(5) Moreover, the preventive measures of γ coarse grain utilizing high speed and high current ESW or welding materials yielding high δ content could be interpreted from their TZT diagrams.

Acknowledgement

The authors would like to thank Mitsubishi Heavy Industries for the execution of actual overlaying.

References

1) W. F. Savage, et al.: Weld. J., **55** (1976), 260s.
2) K. Naitoh, et al.: JHPI, **18** (1980), p. 263 (in Japanese).
3) K. Naitoh, et al.: JHPI, **18** (1980), p. 271 (in Japanese).
4) T. Sakai, et al.: Weld. Met. Committee, Japan Weld. Soc., WM-889-82, 1982 (in Japanese).
5) K. Yasuda, et al.: Weld. Met. Committee, Japan Weld. Soc., WM-891-82, 1982 (in Japanese).
6) T. Ohnishi, et al.: Quarterly J., Japan Weld. Soc., **1** (1983), p. 377 (in Japanese).
7) T. Ohmae, et al.: Weld. Met. Committee, Japan Weld. Soc., WM-974-84, 1984 (in Japanese).
8) R. Kume, et al.: Weld. Met. Committee, Japan Weld. Soc., WM-973-84, 1984 (in Japanese).
9) K. Yasuda and S. Nakano: J. Japan Weld. Soc., **54** (1985), p. 438 (in Japanese).
10) Y. Kikuta, et al.: Quarterly J. Japan Weld. Soc., **2** (1984), p. 463 (in Japanese).
11) F. Matsuda and H. Nakagawa: Trans. JWRI, **13** (1984), p. 159.
12) F. Matsuda, et al: Trans. JWRI, **13** (1984), p. 263.
13) K. Ohnishi: J. Japan Weld. Soc., **54** (1985), p. 154 (in Japanese).
14) T. Araki: J. Japan Weld., Soc., **54** (1985), p. 396 (in Japanese).
15) T. Imanaka, et al.: Committee of Welding Special Mater. Japan Weld. Engineering Soc., SWD-59-21, 1985 (in Japanese).
16) A. Fuji, et al.: Quarterly J. Japan Weld. Soc., 4 (1986), p. 399 (in Japanese).
17) K. Hashimoto, et al.: J. Japan Iron & Steel Inst., **72** (1986), p. 2271 (in Japanese).
18) F. Matsuda, et al.: Trans. JWRI, **15** (1986), p. 379.
19) V. G. Rivin and G. V. Raynor: Int. Met. Rev., 1980, No. 1, p. 21.
20) J. C. Lippold and W. F. Savage: Weld. J., **58** (1979), 362s.
21) G. L. Leone and H. W. Kerr: Weld. J., **61** (1982), 13s.
22) J. M. Vitek, et al.: Met. Trans., 14A (1983), p. 1833.
23) S. Katayama and A. Matsunawa: ICALEO, **44** (1984), p. 60.
24) Kawasaki Steel Corp.: Patent J., Japan, 4971, 1984.